[AU : QA1] [AU : 1] [AU : 2] [AU : 3]

Transcription Factor ATAF1 Integrates Carbon Starvation Responses with Trehalose Metabolism[1][OPEN]

Prashanth Garapati, Regina Feil, John Edward Lunn, Patrick Van Dijck, Salma Balazadeh*, and Bernd Mueller-Roeber*

Institute of Biochemistry and Biology, University of Potsdam, 14476 Potsdam-Golm, Germany (P.G., S.B., B.M.-R.); Plant Signaling Group (P.G., S.B., B.M.-R.) and System Regulation Group (R.F., J.E.L.), Max Planck Institute of Molecular Plant Physiology, 14476 Potsdam-Golm, Germany; and Department of Molecular Microbiology, VIB and Laboratory of Molecular Cell Biology, KU Leuven, B–3001 Leuven, Belgium (P.V.D.)

ORCID ID: 0000-0002-1542-897X (P.V.D.).

[AU : 5] [AU : 6] [AU : 7] Plants respond to low carbon supply by massive reprogramming of the transcriptome and metabolome. We show here that the carbon starvation-induced NAC transcription factor *ATAF1* from Arabidopsis (*Arabidopsis thaliana*) plays an important role in this physiological process. We identified *TREHALASE1*, the only trehalase-encoding gene in Arabidopsis, as a direct downstream target of ATAF1. Overexpression of ATAF1 activates *TREHALASE1* expression and leads to reduced trehalose-6-phosphate levels and a sugar starvation metabolome. In accordance with changes in expression of starch biosynthesis- and breakdown-related genes, starch levels are generally reduced in *ATAF1* overexpressors but elevated in *ataf1* knockout plants. At the global transcriptome level, genes affected by ATAF1 are broadly associated with energy and carbon starvation responses. Furthermore, transcriptional responses triggered by ATAF1 largely overlap with expression patterns observed in plants starved for carbon or energy supply. Collectively, our data highlight the existence of a positively acting feedforward loop between *ATAF1* expression, which is induced by carbon starvation, and the depletion of cellular carbon/energy pools that is triggered by the transcriptional regulation of downstream gene regulatory networks by ATAF1.

Trehalose is a nonreducing disaccharide formed by an α,α-1,1-glucoside bond between two α-Glc units, and it is found in a wide range of organisms (Avonce et al., 2006). Trehalose biosynthesis involves trehalose-6-P synthases (TPSs) and trehalose-6-P phosphatases (TPPs), which catalyze the consecutive generation of trehalose-6-P (Tre6P) from Glc-6-P and UDP-Glc and the dephosphorylation of Tre6P to trehalose. The Arabidopsis (*Arabidopsis thaliana*) genome contains 11 *TPS* genes, of which *TPS1* (Blázquez et al., 1998) as well as *TPS2* and *TPS4* (Delorge et al., 2015) encode catalytically active enzymes, whereas all 10 *TPP* genes encode active enzymes conferring spatiotemporal control over trehalose metabolism (Vandesteene et al., 2012). Trehalose is catabolized into two Glc monomers by trehalase, a plasma membrane-associated enzyme with its catalytic domain oriented toward the apoplast (Frison et al., 2007). In Arabidopsis, trehalase is encoded by a single gene (*TREHALASE1* [*TRE1*]; Leyman et al., 2001; Müller et al., 2001; Lunn, 2007). The level of Tre6P reflects Suc concentration and has been widely accepted as a signal for Suc status in plants (Lunn et al., 2006, 2014). Tre6P is necessary for carbon utilization and growth, although the molecular mechanisms through which it regulates plant growth are not known in detail (Schluepmann et al., 2003, 2012; Zhang et al., 2009; Martins et al., 2013; Yadav et al., 2014).

Snf1-related kinase1 (SnRK1) is the plant homolog of [AU : 8] the yeast (*Saccharomyces cerevisiae*) Snf1 protein kinase and animal AMP-activated protein kinases, and it consists of the three subunits α, β, and γ (Halford and Hey, 2009). In Arabidopsis, the catalytic α-subunit is encoded by two homologous genes (i.e. *KIN10* and [AU : 9] *KIN11*). Transient overexpression of *KIN10* in protoplasts causes massive transcriptional reprogramming, which resembles expressional patterns induced by sugar starvation, indicating that SnRK1 plays a role in mediating the energy deficiency response by repressing anabolic processes that utilize carbon to promote growth (Baena-González et al., 2007). In addition, accumulation of Tre6P in response to high Suc levels has been proposed to inhibit SnRK1 activity in developing

[1] This work was supported by the Deutsche Forschungsgemeinschaft (FOR 948; grant nos. MU 1199/14–2 and BA4769/1–2), the Fund for Scientific Research Flanders, and the International Max Planck Research School Primary Metabolism and Plant Growth (fellowship to P.G.).

* Address correspondence to balazadeh@mpimp-golm.mpg.de and bmr@uni-potsdam.de.

[AU : 4] The author responsible for distribution of materials integral to the findings presented in this article in accordance with the policy described in the Instructions for Authors (www.plantphysiol.org) is: Bernd Mueller-Roeber (bmr@uni-potsdam.de).

P.G. performed most of the experiments and analyzed the data; R.F. and J.E.L. quantified the primary metabolites and Tre6P; P.V.D. provided the anti-TRE1 antibody and gave advice for performing the Western blot experiment; S.B. and B.M.-R. conceived the project and wrote the article, with contributions from P.G., P.V.D., and J.E.L.

[OPEN] Articles can be viewed without a subscription.

www.plantphysiol.org/cgi/doi/10.1104/pp.15.00917

tissues (Zhang et al., 2009; Paul et al., 2010); whether this inhibition operates in a simple linear manner or as part of a more complex regulatory network is a matter of debate (Lunn et al., 2014). Of note, transcription [AU : 10] factors, including the NAC family member ATAF1 and [AU : 11] the ABI3VP1 family protein FUSCA3, interact with SnRK1 (Kleinow et al., 2009; Tsai and Gazzarrini, 2012); however, the physiological role of these interactions is unknown at present.

ATAF1 has been reported to negatively regulate the expression of stress-responsive genes in drought-stressed plants and upon treatment with the phyto- [AU : 12] hormone abscisic acid (ABA), and an involvement in the physiological response to drought stress has been described (Lu et al., 2007; Jensen et al., 2008; Wu et al., 2009). In one study, overexpression of *ATAF1* in transgenic Arabidopsis plants led to enhanced drought tolerance (Wu et al., 2009), whereas earlier studies reported a superior drought tolerance in *ataf1* knockout mutants (Lu et al., 2007; Jensen et al., 2008), suggesting that the response to drought might be affected by additional physiological parameters. As shown by Jensen et al. (2013), ATAF1 is a direct upstream transcriptional [AU : 13] regulator of *NCED3*, which encodes a key enzyme of ABA biosynthesis. In accordance with this, overexpression of ATAF1 enhances *NCED3* expression and triggers an increase in ABA level, whereas *NCED3* transcript abundance was found to be lowered in *ataf1* knockout mutants compared with the wild type. The increased drought tolerance observed by Wu et al. (2009) for *ATAF1* overexpressors is in line with a regulatory effect of ATAF1 on *NCED3*. Other known direct targets of ATAF1 are the *ORE1* and *GLK1* transcription [AU : 14] factors (Garapati et al., 2015). *ORE1* (also called *ANAC092*) encodes a key positive regulator (an NAC [AU : 15] transcription factor) of senescence (Kim et al., 2009; Balazadeh et al., 2010), whereas GLK1 is an important transcriptional regulator (other than GLK2) of chloroplast development and maintenance (Waters et al., 2008, 2009). Notably, although ATAF1 positively affects the expression of *ORE1*, it negatively regulates the expression of *GLK1*, thereby promoting senescence (Garapati et al., 2015). In accordance with its function as a positive regulator of senescence, *ATAF1* expression increases during developmental and salinity stress-induced leaf senescence (Balazadeh et al., 2008; Allu et al., 2014).

Here, we show that ATAF1 directly regulates the expression of *TRE1* and induces global transcriptomic changes that largely overlap with expression profiles

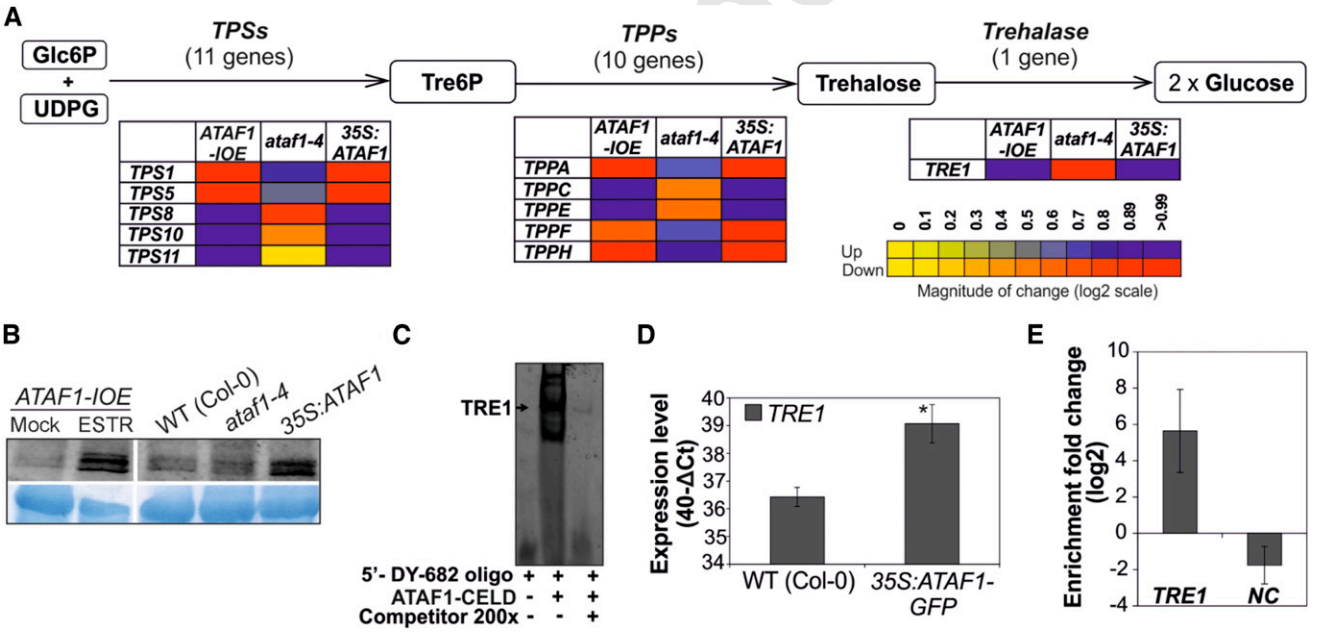

Figure 1. *TRE1* is a direct target of ATAF1. A, Expression of trehalose metabolism-related genes after 5 h of ESTR induction in *ATAF1-IOE* (compared with mock), *ataf1-4* (compared with the wild type), and *35S:ATAF1* (compared with the wild type) plants. Heat maps indicate $\log_2$ fold change expression ratios relative to controls. Means of three biological replicates each were determined in two technical replicates. Full data are given in Supplemental Table S1. B, Immunoblot analysis of TRE1 accumulation in extracts from 2-week-old *ATAF1-IOE* seedlings (treated with 10 μM ESTR for 10 h; mock: 0.1% ethanol), the wild type (WT), *ataf1-4*, and *35S:ATAF1*; Coomassie Brilliant Blue stain shows Rubisco large subunit as control. C, EMSA confirms binding of ATAF1 to its binding site in the *TRE1* promoter. D, *TRE1* expression in 2-week-old *35S:ATAF1-GFP* seedlings compared with the wild type. Data represent means of two biological replicates each determined in three technical replicates. *, Statistically significant difference to the wild type ($P < 0.05$; Student's *t* test). E, ChIP-qPCR confirms in vivo binding of ATAF1 to *TRE1* promoter. [AU : 45] Primers span the ATAF1 binding site. As negative control, primers annealing to a promoter region of a gene (*CLV1*) lacking an ATAF1 binding site were used. Mean ± SD ($n = 3$). G6P, Glc-6-P; UDPG, UDP-Glc.

observed in carbon- or energy-starved plants and are similar to the SnRK1-induced carbon starvation response. Our results thus provide a molecular link between physiological processes triggered by energy deficiency and downstream transcriptional output to adjust plant growth and physiology.

RESULTS AND DISCUSSION

ATAF1 Regulates Trehalose Metabolism

To identify target genes of ATAF1, we generated transgenic Arabidopsis plants expressing *ATAF1* under the control of a chemically (estradiol [ESTR]) inducible promoter (*ATAF1-IOE* lines) and performed transcriptome profiling using Affymetrix ATH1 microarrays on samples harvested 1, 2, and 5 h after ESTR induction (for experimental details, see "Materials and Methods"). Several genes encoding enzymes of trehalose metabolism were found to be transcriptionally affected. To confirm this observation, we reassessed the expression of trehalose metabolism-related genes by quantitative reverse transcription (qRT)-PCR in 2-week-old *ATAF1-IOE* seedlings after 5 h of ESTR treatment as well as in *35S:ATAF1* overexpressors and a transfer DNA insertion line (homozygous *ataf1-4* knockout mutant from the GABI-Kat Collection; GK565H08). As seen in Figure 1A and Supplemental Table S1, expressions of *TPS1*, *TPS5*, *TPP-A*, *TPP-F*, and *TPP-H* were reduced, whereas expressions of *TPS8*, *TPS10*, *TPS11*, *TPP-C*, *TPP-E*, and *TRE1* were elevated in ESTR-treated *ATAF1-IOE* seedlings and *35S:ATAF1* plants. The opposite was observed in *ataf1-4*, indicating that ATAF1 plays a role in transcriptional regulation of the synthesis and breakdown of intermediates of trehalose metabolism. We, therefore, determined the levels of Tre6P and its substrates in seedlings of wild-type and *ATAF1*-modified plants. The level of Tre6P was significantly reduced in *35S:ATAF1* but increased in *ataf1-4* compared with the wild type (Fig. 2A). The levels of UDP-Glc and Glc-6-P, the substrates for Tre6P synthesis, also had a contrasting pattern in *35S:ATAF1* and *ataf1-4* plants compared with the wild type (Fig. 2, B and C).

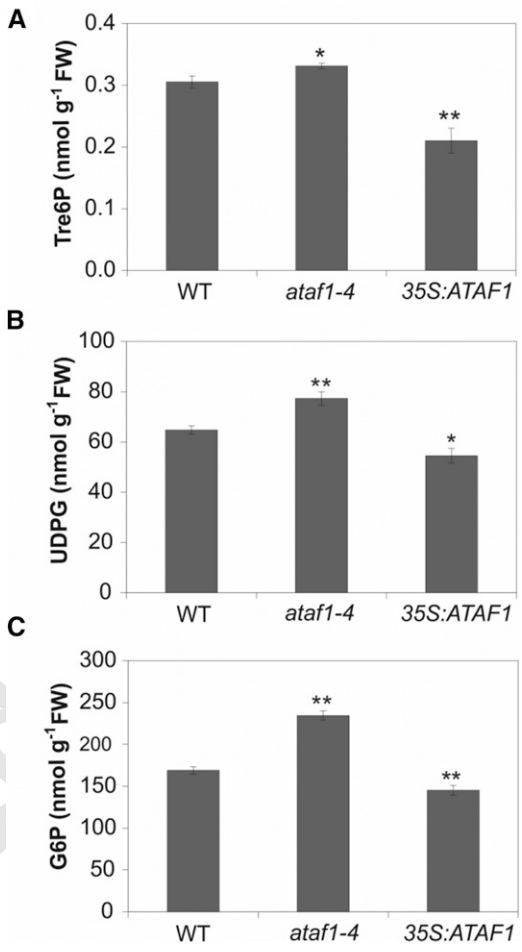

Figure 2. Levels of Tre6P (A), UDP-Glc (UDPG; B), and Glc-6-P (G6P; C) in wild-type (WT), *ataf1-4*, and *35S:ATAF1* seedlings. Two-week-old wild-type, *ataf1-4*, and *35S:ATAF1* seedlings grown on solid one-half-strength Murashige and Skoog medium supplemented with 1% (w/v) Suc were harvested for metabolite determinations. Data represent mean ± SD (three replicates with 10 seedlings each). Asterisks indicate statistically significant differences to the wild type (*, $P < 0.05$; **, $P < 0.01$; Student's *t* test). FW, Fresh weight.

TRE1 Is a Direct ATAF1 Target

Overexpression of *ATAF1* led to increased *TRE1* expression (Fig. 1A) and trehalase protein level (Fig. 1B). Analysis of the promoters of trehalose metabolism-related genes revealed the presence of an ATAF1 binding site [VDHVNNYRR(N_6)YACGNMWSK] in *TRE1* at positions −561 to −538 bp upstream of the transcription start site, suggesting it to be a direct downstream target of ATAF1. To test this possibility, we performed an EMSA and observed binding of ATAF1 to a double-stranded DNA probe containing the ATAF1 binding site of the *TRE1* promoter (Fig. 1C). To provide additional evidence of in vivo regulation of *TRE1* by ATAF1, we performed chromatin immunoprecipitation (ChIP) using a transgenic line that expresses the ATAF1-GFP fusion protein under control of the cauliflower mosaic virus 35S promoter. Elevated *TRE1* expression was observed in the *35S:ATAF1-GFP* line (Fig. 1D), confirming that the fusion protein was functional, and an enrichment of *TRE1* promoter fragments in the precipitated chromatin was determined by quantitative PCR (qPCR) using primers spanning the ATAF1 binding site (Fig. 1E).

Growth of *ATAF1*-Modified Plants on Trehalose Medium

Trehalose leads to toxic effects when present at high concentration in the medium (Schluepmann et al., 2004). In Arabidopsis, seedlings fail to develop rosette

leaves and exhibit stunted root growth when grown on medium supplemented with trehalose; this effect is even more pronounced in *tre1* knockout mutants, whereas *TRE1* overexpressors show improved growth, likely because of the capacity of the apoplastic trehalase to catabolize external trehalose, thereby avoiding toxicity (Van Houtte et al., 2013). Because expression of *TRE1* was reduced in *ataf1-4* but enhanced in *35S:ATAF1* plants, we tested their growth on trehalose-containing medium, revealing reduced root

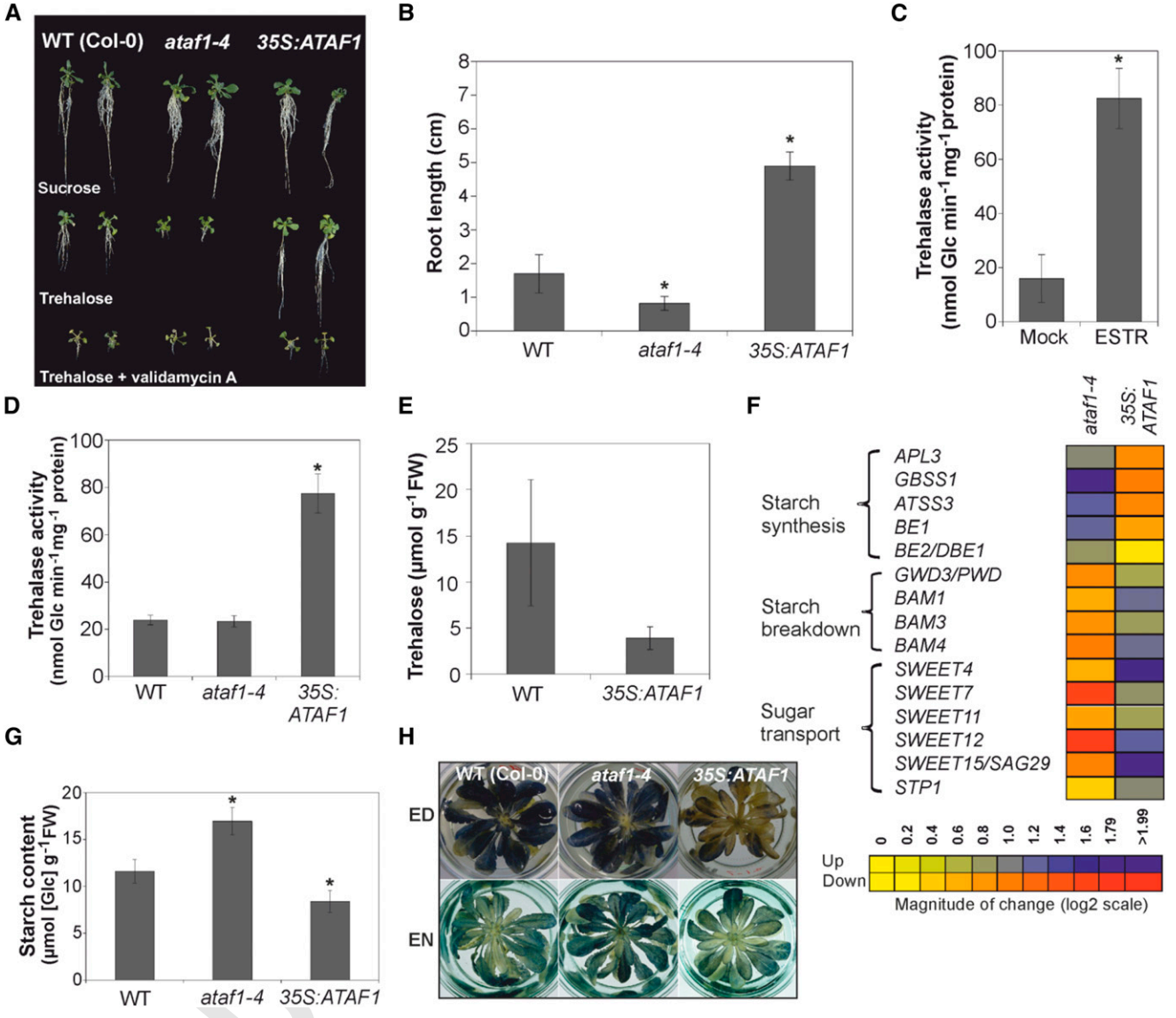

Figure 3. Plant growth and starch accumulation. A, Seedlings grown for 2 weeks on one-half-strength Murashige and Skoog medium and 1% (w/v) Suc (29.2 mM) were transferred to one-half-strength Murashige and Skoog medium supplemented with Suc (29.2 mM), trehalose (25 mM), or trehalose (25 mM) and validamycin A (10 μM) and grown for 2 more weeks. Note the difference in root growth on trehalose medium. B, Root length of seedlings 2 weeks after transfer to trehalose (25 mM) medium ($n = 6$). C, Trehalase activity in *ATAF1-IOE* seedlings treated with ESTR (10 μM) or mock (0.1% [v/v] ethanol) for 10 h. D, Trehalase activity in wild-type (WT), *ataf1-4* mutant, and *35S:ATAF1* seedlings transferred to trehalose (25 mM) medium and grown for 10 d. Note higher trehalase activity upon *ATAF1* overexpression in C and D. E, Trehalose content in wild-type and *35S:ATAF1* seedlings grown on trehalose (25 mM) medium for 10 d. F, Heat map of expression of starch metabolism- and sugar transport-related genes. Gene expression was determined in 10-d-old seedlings grown on plates at 12 h into the light period (which was 16 h in total). Means of three biological replicates each were determined in two technical replicates. Full data are given in Supplemental Table S1. G, Starch content in shoots of seedlings grown for 10 d on trehalose (25 mM) medium. Samples were harvested in the middle of the 16-h-light period. H, Lugol staining of rosettes of soil-grown plants (12-h photoperiod) at ED and EN. Note the reduced staining of *35S:ATAF1* rosette at ED and EN. Data in graphs represent mean ± SD of three biological replicates with 10 seedlings each. FW, Fresh weight. *, Significant difference to controls ($P < 0.05$; Student's *t* test).

[AU : 48]

elongation in *ataf1-4* seedlings but increased elongation in *35S*:*ATAF1* seedlings compared with the wild type (Fig. 3, A and B). Notably, the enhanced root growth of *35S*:*ATAF1* plants was suppressed on trehalose medium supplemented with validamycin A, an inhibitor of trehalase, suggesting that increased root elongation was triggered by enhanced trehalase activity compared with controls, which we, indeed, observed in ESTR-induced (10 h) *ATAF1-IOE* and *35S*:*ATAF1* seedlings (Fig. 3, C and D). Concomitant with elevated trehalase activity in these lines, trehalose levels were reduced in *35S*:*ATAF1* seedlings compared with the wild type grown on trehalose medium (Fig. 3E).

Shoots of trehalose-grown seedlings accumulate starch likely because of (1) transcriptional induction of [AU : 23] *APL3* that encodes one of four isoforms of the large subunit of ADP-Glc pyrophosphorylase, a key enzyme of starch biosynthesis (Ekkehard Neuhaus and Stitt, 1990; Vigeolas et al., 2004), and (2) an impaired export of Suc to sinks (Wingler et al., 2000). Furthermore, inhibition of root growth on trehalose correlates with impaired expression of genes involved in starch breakdown, such as *STARCH EXCESS1* (*SEX1*) and *β-AMYLASE3* (*BAM3*), and the *SUGAR TRANSPORTER1* (*STP1*) gene, resulting in altered sugar allocation to or perception in the root (Ramon et al., 2007).

To test a possible function of ATAF1 in this process, [AU : 24] we measured the expressions of starch synthesis- (*APL3*, *GBSS1*, *SS3*, *BE1*, and *ISA2/DBE1*), starch breakdown- (*GWD3*, *BAM1*, *BAM3*, and *BAM4*), and sugar transport-related genes (*SWEET4*, *SWEET7*, *SWEET11*, *SWEET12*, *SWEET15*, and *STP1*) in *ATAF1* plants grown on trehalose medium. As shown in Figure 3F, genes encoding enzymes of starch biosynthesis showed elevated expression, whereas genes linked to starch breakdown and sugar transport were decreased in *ataf1-4* shoots compared with the wild type, and opposite patterns occurred in *35S*:*ATAF1*. The observed expression profiles suggested altered starch turnover. Indeed, starch content in *ataf1-4* seedlings grown on trehalose medium for 10 d was higher than in the wild type and reduced in *35S*:*ATAF1* seedlings (Fig. 3G; starch determined at midday).

We next determined starch in rosette leaves of plants grown in soil with a 12-h photoperiod. At the end of the day (ED), starch levels were lower in *35S*:*ATAF1* than the wild type, whereas there was no difference between *ataf1-4* and the wild type. However, at the end of the night (EN), *ataf1-4* plants retained slightly more starch than the wild type, likely because of ATAF1-induced changes in starch metabolism (Fig. 3H; Supplemental Fig. S1), in accordance with the expression of native *ATAF1*, which is higher at EN than ED in the wild type.

The above-reported changes in starch accumulation in *ATAF1*-modified plants not only might be caused by transcriptional control exerted by ATAF1 over starch biosynthesis and breakdown-related genes but also, might involve Tre6P itself as a regulatory molecule, which has been proposed to negatively affect starch breakdown, although the biochemical mechanism through which this control is exerted remains unknown at present (Martins et al., 2013).

It was previously reported that overexpression of *KIN10* or the transcription factor *bZIP11* confers [AU : 25]

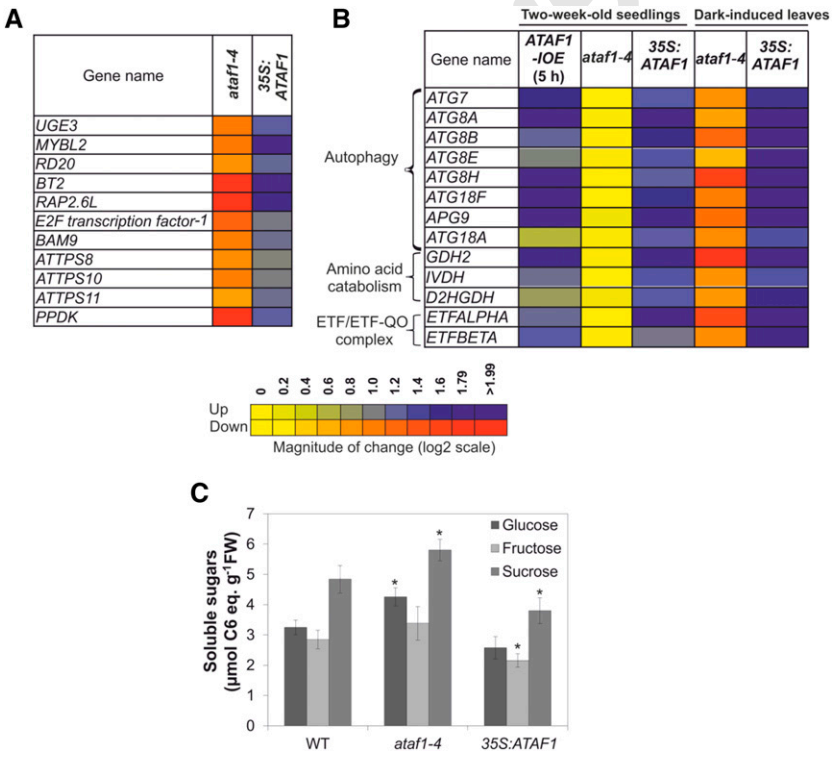

Figure 4. Gene expression and sugar levels. A, Heat map of expression of *KIN10*-regulated genes in shoots of *ATAF1* transgenic seedlings compared with the wild type (WT). Gene expression analysis was performed on shoots of seedlings grown in trehalose (25 mM) medium for 10 d. B, Heat map of gene expression determined by qRT-PCR in seedlings or detached leaves of 3-week-old soil-grown plants subjected to dark incubation on moist filter paper for 3 d. Differences to controls (mock treatment for *ATAF1-IOE* and the wild type for *35S*:*ATAF1* and *ataf1-4* plants) are shown. Data in A and B are means of three biological replicates (each determined in two technical replicates). C, Sugar levels in seedlings grown for 2 weeks on one-half-strength Murashige and Skoog medium and 1% (w/v) Suc medium. Mean ± SD (three replicates with 10 seedlings each). Full data for A and B are given in Supplemental Table S1. ETF/ETF-QO, Electron transfer flavoprotein/electron [AU : 49] transfer flavoprotein:ubiquinone oxidoreductase; FW, fresh weight. *, Significant difference from controls ($P < 0.05$; Student's t test).

trehalose resistance without a significant induction of trehalase activity (Delatte et al., 2011), which differs from the situation shown here for *ATAF1* overexpressors exhibiting elevated trehalase activity. Together, these observations suggest that trehalase contributes but may not be the only factor supporting tolerance to exogenously supplied trehalose.

ATAF1 Induces a Carbon Starvation Transcriptome

It was shown earlier that transient overexpression of *KIN10* (encoding the α-subunit of SnRK1) in protoplasts causes transcriptional reprogramming with 506 up- and 515 down-regulated genes (2-fold cutoff); the expression pattern resembled that of sugar-starved cells (Baena-González et al., 2007). Because *ATAF1* overexpressors had decreased levels of Tre6P, possibly signaling low Suc availability (Lunn et al., 2006, 2014), we compared the transcriptome data of ESTR-treated *ATAF1-IOE* seedlings and mature leaves with the 1,021 genes modified by *KIN10* overexpression. As shown in Supplemental Figure S2, the number of KIN10-affected genes increased over time in *ATAF1-IOE* samples (Supplemental Table S2). Thus, the *ATAF1-IOE* transcriptome became progressively more similar to the SnRK1-induced expression profile, which resembles carbon starvation-induced transcript profiles (Baena-González et al., 2007).

Furthermore, we tested the expression of a subset of randomly chosen genes that are up-regulated by both *ATAF1* and *KIN10* overexpression in seedlings transferred onto trehalose medium. As shown in Figure 4A, the expression of SnRK1 up-regulated genes was elevated in *35S:ATAF1* seedlings, whereas their expression was reduced in *ataf1-4* compared with the wild type, showing an up-regulation of SnRK1-mediated transcriptional responses upon *ATAF1* overexpression. Thus, *35S:ATAF1* seedlings seem to adopt a transcriptional status similar to that of protoplasts transiently overexpressing SnRK1.

Previously, global transcriptional responses to changes of endogenous sugar availability were identified by comparing Arabidopsis plants illuminated for 4 [AU : 26] h at ambient or low ($<50\ \mu L\ L^{-1}$) CO_2 concentration (Bläsing et al., 2005). Because *ATAF1* was among the genes strongly repressed at ambient CO_2 (supplemental table S6M in Bläsing et al., 2005; Supplemental Fig. S3), we compared the ATAF1-induced transcriptional responses with the top 200 genes induced or repressed upon carbon fixation (Bläsing et al., 2005). As seen in Figure 5 (Supplemental Table S3), genes induced by carbon fixation were repressed in *ATAF1-IOE* and vice versa.

We next compared the ATAF1-controlled genes with (1) genes affected by the addition of Suc (15 mM; 30 min and 3 h) or Glc (100 mM; 3 h) to carbon-starved seedlings (Bläsing et al., 2005; Osuna et al., 2007) and (2) genes that are altered at ED (carbon rich) compared with EN (carbon poor) in Columbia-0 (Col-0) wild-type

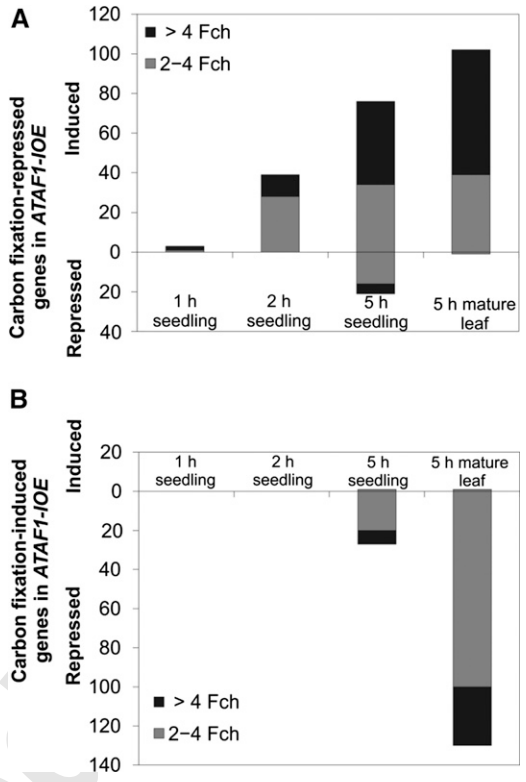

Figure 5. Number of carbon fixation-responsive genes differentially expressed in *ATAF1-IOE* upon ESTR induction. A, Genes repressed by carbon fixation that are induced in *ATAF1-IOE*. Note that the number of carbon fixation-repressed genes that are induced in *ATAF1-IOE* increases with extended ESTR induction times. B, Genes induced by carbon fixation that are repressed in *ATAF1-IOE*. Note that the number of carbon fixation-induced genes that are repressed in *ATAF1-IOE* increases with extended ESTR induction times. Carbon fixation-responsive genes were taken from Bläsing et al., 2005. Fch, Fold change.

and starch-deficient *phosphoglucomutase* mutant plants [AU : 27] (Bläsing et al., 2005). Notably, genes repressed by carbon resupply/high energy status of the plant are induced in *ATAF1-IOE* overexpressors (Fig. 6A), whereas conversely, genes induced by carbon readdition/high energy status are repressed (Fig. 6B; Supplemental Table S4). Furthermore, genes induced or repressed by *ATAF1* overexpression largely overlap with genes induced or repressed, respectively, under conditions of extended night (Usadel et al., 2008; Fig. 6C; Supplemental Table S5). Thus, the transcriptome data clearly indicate that ATAF1 induces a transcriptional reprogramming that is highly similar to gene expression changes observed under conditions of carbon or energy limitation.

To gain a wider insight into the cellular processes affected by ATAF1, we clustered the genes affected by its expression within 1 to 5 h of ESTR treatment (in *ATAF1-IOE* lines) using the Short Time-Series Expression Miner (STEM; Ernst and Bar-Joseph, 2006). STEM analysis identified three significant clusters with genes up-regulated over time (profiles 13, 8, and 12) and three

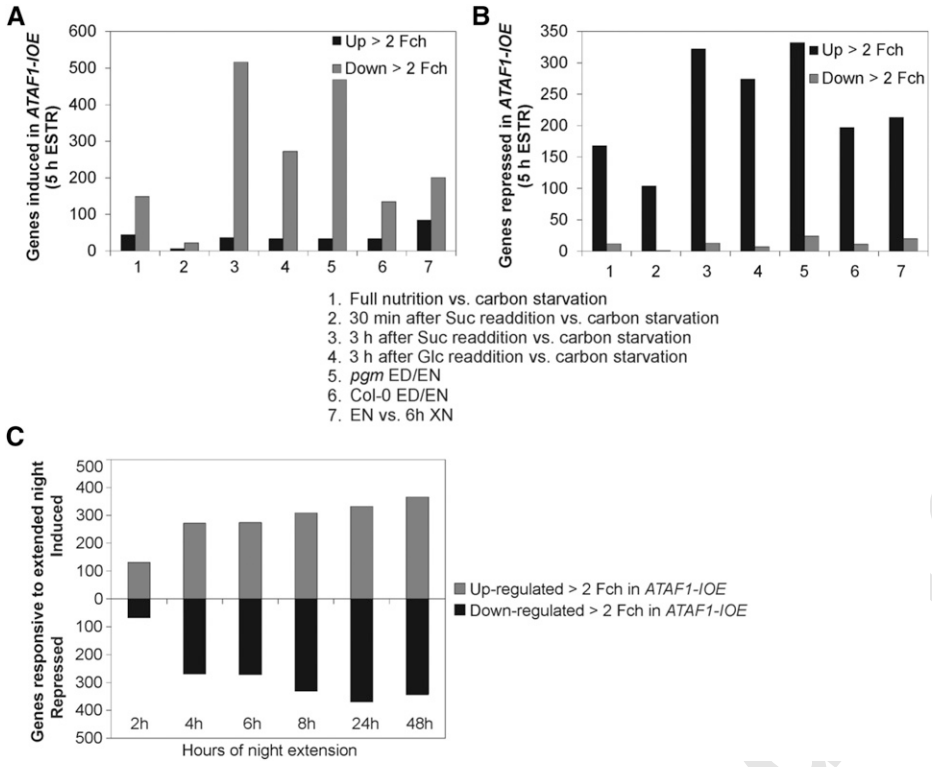

Figure 6. Number of carbon/energy status-responsive genes differentially expressed in *ATAF1-IOE* upon ESTR induction. A, Genes up- or down-regulated by at least 2-fold in various carbon readdition experiments (nos. 1–4; Bläsing et al., 2005; Osuna et al., 2007) and high-energy status experiments (nos. 5–7; Thimm et al., 2004; Bläsing et al., 2005) were compared with genes induced after 5 h of ESTR induction in leaves of 30-d-old *ATAF1-IOE* plants. Note that the vast majority of the genes repressed by carbon resupply/high energy status were induced in *ATAF1-IOE*. B, The genes up- or down-regulated by at least 2-fold in the various carbon starvation experiments were compared with genes repressed after 5 h of ESTR induction. Note that the vast majority of the genes induced by carbon resupply/high energy status were repressed in *ATAF1-IOE*. C, Genes affected by extended darkness (Usadel et al., 2008) and expressed differentially in *ATAF1-IOE*. Fch, Fold change; *pgm*, *phosphoglucomutase* mutant; XN, extended night.

clusters with genes down-regulated (profiles 7, 2, and 3) after *ATAF1* induction (Supplemental Fig. S4A; [AU : 28] Supplemental Table S6). Analysis of the GO terms significantly associated with genes in the up-regulated profiles include response to water deprivation, autophagy, galactolipid metabolic process, and cellular response to phosphate starvation (Supplemental Fig. S4B), whereas those associated with genes down-regulated by ATAF1 include carbohydrate biosynthetic process, sulfur compound biosynthetic process, pentose-P shunt, and starch biosynthetic process (Supplemental Fig. S4C). Thus, the observed transcriptome responses further support the notion that ATAF1 induces a physiological response reminiscent of carbon or energy deprivation.

Autophagy and Amino Acid Catabolism Genes Are Up-Regulated by ATAF1

Autophagy is a cellular process that results in the degradation of cytoplasmic components upon carbon starvation (Contento et al., 2004; Avin-Wittenberg et al., 2015), concomitant with the induction of autophagy- [AU : 29] related genes, such as *ATG3*, *ATG4a*, *ATG4b*, *ATG7*, and *ATG8a* to *ATG8i* in Arabidopsis (Rose et al., 2006). Likewise, genes encoding enzymes involved in amino acid breakdown, such as isovaleryl-CoA dehydrogenase, D-2-hydroxyglutarate dehydrogenase, and Glu dehydrogenase, and genes encoding mitochondrial electron transfer flavoprotein/electron transfer flavoprotein:ubiquinone oxidoreductase subunits are up-regulated upon carbon limitation (Ishizaki et al., 2006; Miyashita and Good, 2008; Araújo et al., 2011; Izumi et al., 2013). Isovaleryl-CoA dehydrogenase and D-2-hydroxyglutarate dehydrogenase act as electron donors to the electron transfer flavoprotein/electron transfer flavoprotein:ubiquinone oxidoreductase-mediated alternative pathway of respiration (Araújo et al., 2010). Thus, during sugar starvation, autophagy contributes to amino acid catabolism, thereby allowing use of free amino acids as alternative respiratory substrates.

To confirm the molecular carbon starvation phenotype of *ATAF1* transgenic lines, we used qRT-PCR to test the expressions of genes of all three metabolic pathways and observed strong induction in *ATAF1-IOE* and *35S:ATAF1* plants, whereas expressions of the tested genes were not significantly different between *ataf1-4* and the wild type (Fig. 4B; Supplemental Table S1). However, expressions of these genes were reduced in dark-incubated leaves of soil-grown *ataf1-4* mutants compared with the wild type (Fig. 4B), suggesting that loss of *ATAF1* results in a delayed launch of autophagy, which is in accordance with the delayed dark-induced senescence of *ataf1* knockout mutants (including *ataf1-4*) as previously reported (Garapati et al., 2015).

ATAF1 Triggers Suc Starvation-Type Changes in Primary Metabolism

Previous research showed that sugars and glycolytic intermediates are depleted in carbon-starved seedlings, whereas their levels increase after Suc resupply (Lunn et al., 2006). It was also shown that Tre6P controls primary metabolism and is essential for carbohydrate utilization and plant growth (Schluepmann et al., 2003). Because *ATAF1*-modified plants showed altered levels of Tre6P, we investigated whether perturbed expression of *ATAF1* has an influence on central sugar metabolism by measuring primary metabolites in seedlings of wild-type and *ATAF1*-modified plants (Table I). The levels of glycolytic intermediates were higher in the *ataf1-4* mutant and lower in *35S:ATAF1* plants compared with the wild type. Additionally, the levels of soluble sugars (Glc, Fru, and Suc) were lower and higher in *35S:ATAF1* and *ataf1-4* plants, respectively (Fig. 4C). Thus, the metabolic changes in *35S:ATAF1* plants mimic those occurring during Suc starvation (Lunn et al., 2006).

Model of ATAF1 Action

Based on the data presented here and elsewhere (Bläsing et al., 2005; Baena-González et al., 2007; Zhang et al., 2009; Paul et al., 2010; Lunn et al., 2014; Yadav et al., 2014), we propose a model for the regulatory integration of ATAF1 (Fig. 7). Expression of *ATAF1* is strongly induced by carbon limitation triggered by environmental input (e.g. an extended night [Usadel et al., 2008], dark incubation of whole plants [Lin and Wu, 2004; Garapati et al., 2015], drought stress [Lu et al., 2007; Wu et al., 2009], or low atmospheric CO_2 concentration [Bläsing et al., 2005]), leading directly and indirectly to reprogramming of the transcriptome and metabolome. This response includes the direct transcriptional activation of the *TRE1* gene by ATAF1. In addition, ATAF1 may act through transcriptional regulation of other carbon metabolism-related genes (compare with Fig. 3F). Enhanced expression of *ATAF1* triggers a reduction of cellular trehalose, Tre6P, Suc, and starch levels. Low carbon status may, furthermore, act through currently unknown mechanisms by which low carbon (potentially Suc) inhibits TPS1 or activates TPP as suggested previously (Yadav et al., 2014). ATAF1 might also lead to transcriptional reprogramming by reducing cellular Tre6P level and a concomitant activation of SnRK1 protein kinase activity (indicated as SnRK1 regulation in Fig. 7), although it currently remains unknown how exactly Tre6P and

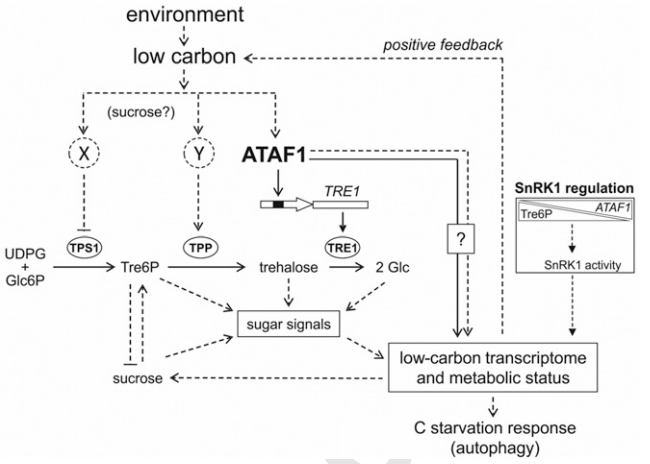

Figure 7. Model of ATAF1 action. Reduced carbon availability triggered by environmental input (e.g. extended darkness, low atmospheric CO_2 concentration, or drought) induces *ATAF1* expression, whereas high expression of ATAF1 itself causes a low-carbon physiological status, suggesting the existence of a carbon starvation feedforward loop that involves ATAF1 as a regulatory node. ATAF1 directly up-regulates expression of *TRE1* by binding to its promoter and additionally affects the expression of many other carbon starvation-related genes directly or indirectly (indicated by a boxed question mark). X and Y indicate unknown mechanisms by which low carbon (potentially low Suc) inhibits TPS and/or activates TPP, respectively (Yadav et al., 2014). Lines indicate direct regulatory interactions or metabolite conversions, whereas dashed lines indicate interactions of unknown molecular mechanism. Lines with arrows and bars represent activation and repression, respectively. ATAF1 may also lead to transcriptional reprogramming by virtue of the lowered Tre6P level that it induces and a concomitant activation of SnRK1 activity (indicated as SnRK1 regulation) as suggested by others (Zhang et al., 2009; Nunes et al., 2013). G6P, Glc-6-P; UDPG, UDP-Glc.

Table I. *Metabolite concentrations*

Two-week-old wild-type, *35S:ATAF1*, and *ataf1-4* seedlings grown on one-half-strength Murashige and Skoog medium and 1% (w/v) Suc medium were harvested at midday (of a 16-h-light period) for metabolite determinations. Mean ± SD. ADPG, ADP-Glc; F1,6BP, Fru-1,6-bisphosphate; Gly-3P, glycerol-3-P; G1,6BP, Glc-1,6-bisphosphate; 2-OG, 2-oxoglutarate; PEP, phospho*enol*pyruvate; 3-PGA, 3-phosphoglyceric acid. Statistically significant changes (*, $P < 0.05$; **, $P < 0.01$; Student's *t* test) are based on three biological replicates.

Metabolite	Wild Type	*35S:ATAF1*	*ataf1-4*
		nmol g^{-1} fresh weight	
Suc6P	0.24 ± 0.02	0.28 ± 0.01*	0.42 ± 0.01**
Gal6P	2.83 ± 0.40	2.54 ± 0.45	3.55 ± 0.20
G1,6BP	1.45 ± 0.18	1.26 ± 0.09	1.73 ± 0.12
Glc1P	59.1 ± 4.7	55.1 ± 4.2	67.7 ± 1.2
Gly-3P	35.5 ± 6.0	33.2 ± 1.3	70.4 ± 3.8**
PEP	3.82 ± 0.62	4.46 ± 1.33	5.11 ± 1.47
Aconitate	5.51 ± 0.34	7.37 ± 1.66	7.60 ± 1.89
Fru6P	39.3 ± 1.5	35.3 ± 3.7	55.9 ± 2.1**
Man6P	22.4 ± 0.9	17.7 ± 0.5**	28.7 ± 1.6**
F1,6BP	2.75 ± 0.14	1.96 ± 0.47	4.83 ± 0.25**
Shikimate	12.6 ± 1.8	10.6 ± 1.2	16.2 ± 0.5
Isocitrate	2.87 ± 0.4	3.99 ± 0.47*	4.87 ± 0.44**
2-OG	44.5 ± 3.5	50.9 ± 3.4	45.6 ± 0.9
Pyruvate	47.1 ± 2.7	56.0 ± 3.4*	62.5 ± 4.6*
Succinate	60.2 ± 3.1	57.4 ± 2.4	58.2 ± 2.1
3-PGA	61.3 ± 1.7	61.0 ± 7.6	78.0 ± 1.4**
Glycerate	176 ± 4	227 ± 3**	168 ± 39
Citrate	247 ± 18	252 ± 16	367 ± 9**
Malate	758 ± 28	837 ± 60	918 ± 16**
Fumarate	863 ± 24	1,249 ± 41**	922 ± 27*

SnRK1 activities are related in vivo and how SnRK1 controls the expression of genes affected by ATAF1.

In summary, we have identified a positive feedback loop between *ATAF1* expression and the depletion of cellular carbon pools, representing an intriguing example for the control of carbon-related physiology through the integration of transcriptional and metabolic reprogramming. Future work will have to unravel the precise involvement of other transcriptional regulators up- and downstream of ATAF1, including *bZIP11*, which affect trehalose metabolism genes through a currently unknown mechanism (Ma et al., 2011). Evidently, the cellular response to low carbon availability in plants is complex, and ATAF1 plays an important role in the process.

MATERIALS AND METHODS

General

Unless indicated otherwise, chemicals and reagents were obtained from Merck, Invitrogen, Sigma-Aldrich, and Fluka. Molecular biological kits were obtained from Qiagen and Macherey-Nagel. For sequence analyses, the tools provided by the National Center for Biotechnology Information (www.ncbi.nlm.nih.gov), The Arabidopsis Information Resource (http://www.Arabidopsis.org/), the European Bioinformatics Institute (www.ebi.ac.uk), and the Plant Transcription Factor Database (http://plntfdb.bio.uni-potsdam.de/v3.0) were used. QuantPrime (www.quantprime.de) was used for designing qRT-PCR primers, and PatMatch (http://www.arabidopsis.org/cgi-bin/patmatch/nph-patmatch.pl) was used to identify ATAF1 binding sites (details will be published elsewhere) in promoters of trehalose metabolism-related genes. Sequences of oligonucleotides used for qRT-PCR, EMSA, and ChIP-PCR are given in Supplemental Table S7.

Plants

Experiments were performed using wild-type Arabidopsis (*Arabidopsis thaliana*) accession Col-0 (INRA; http://dbsgap.versailles.inra.fr/publiclines) and transgenic plants generated in this background. Seeds of the *ataf1-4* knockout mutant (GK565H08) were obtained from the Nottingham Arabidopsis Stock Centre (http://arabidopsis.info) and genetically characterized before use; the mutant carries a transfer DNA insertion 1,073 bp downstream of the transcription start site in exon 3. For growth under a 12-h photoperiod, seeds were germinated in soil (Einheitserde GS90; Gebrüder Patzer) in a phytotron with a 16-h-light (approximately 120 μE m^{-2} s^{-1} at 20°C)/8-h-dark at 4°C cycle. Two weeks after sowing, seedlings were transplanted to individual 6-cm pots and transferred to equinoctial conditions (12-h-light/12-h-dark cycle) at constant 20°C until harvest. For plate experiments, Arabidopsis seeds were surface sterilized using sodium hypochlorite solution (10%) and sown on nutrient agar medium (full-strength Murashige and Skoog medium and 1% Suc, pH 5.8). The plates were stored for 2 d under stratification condition (16-h-light at 22°C/8-h-dark at 4°C cycle) and then transferred to long-day growth conditions (16-h-light at 22°C/8-h-dark at 18°C cycle).

Constructs

Generation of the constructs was reported by Garapati et al. (2015). In brief, for *35S:ATAF1*, the *ATAF1* open reading frame was inserted through *Pme*I/*Pac*I sites into the pGreen0229-35S plant transformation vector (Skirycz et al., 2006). For *35S:ATAF1-GFP*, the *ATAF1* coding sequence (without stop codon) was fused to the GFP open reading frame in vector pK7FWG2 (Ghent University; http://gateway.psb.ugent.be/vector/show/pK7FWG2/search/index/). The vector carries the *cauliflower mosaic virus 35S* promoter upstream of the *ATAF1-GFP* sequence. For *ATAF1-IOE*, the *ATAF1* coding sequence was inserted through *Xho*I/*Spe*I sites into the pER8 vector (Zuo et al., 2000). *Agrobacterium tumefaciens* strain GV3101 (pMP90) was used for Arabidopsis transformation.

Microarray Analyses

An RNeasy Plant Mini Kit (Qiagen) was used to extract total RNA from 2-week-old *ATAF1-IOE* seedlings that were grown in liquid full-strength Murashige and Skoog medium (1% [w/v] Suc, pH 5.8) and treated with 10 μM ESTR (dissolved in 0.1% [v/v] ethanol; control treatment: 0.1% ethanol) for 1, 2, and 5 h. Alternatively, leaves of 30-d-old plants were incubated for 5 h in liquid one-half-strength Murashige and Skoog medium in the presence of 10 μM ESTR (dissolved in 0.1% [v/v] ethanol; control: 0.1% ethanol) before RNA extraction; 3 μg of RNA was processed for use in Affymetrix ATH1 Microarray Hybridizations. Probe preparation and hybridization were performed by ATLAS Biolabs (http://www.atlas-biolabs.com/). Raw data (CEL files) obtained from RNA hybridization experiments were normalized with the affyPLM package from the Bioconductor Software Project (Gentleman et al., 2004) using GCRMA, and data were normalized with robust multiple array average (Wu et al., 2004). Transcriptional changes were determined by subtracting the normalized signal intensity of the control samples from that of ESTR-induced samples. All four ESTR induction experiments were performed as single-replicate experiments. Clustering of differentially expressed genes (ESTR versus mock treated) was performed using the STEM (http://www.cs.cmu.edu/~jernst/stem; Ernst and Bar-Joseph, 2006). GO annotation was done using the Singular Enrichment Analysis tool from AgriGO (http://bioinfo.cau.edu.cn/agriGO; Du et al., 2010). Expression data are available from the National Center for Biotechnology Gene Expression Omnibus repository (www.ncbi.nlm.nih.gov/geo/) under accession number GSE54676. qRT-PCR using SYBR Green was performed as described (Caldana et al., 2007).

EMSA

For EMSA, recombinant ATAF1-CELD fusion protein (Xue, 2005) was expressed in *Escherichia coli* strain BL21 (DE3) pLysS (Agilent Technologies) as described (Dortay et al., 2011). Protein was purified using Protino Ni-IDA 150 Packed Columns (Macherey and Nagel). EMSA was performed as described (Wu et al., 2012) using the Odyssey Infrared EMSA Kit (Li-Cor; www.licor.com). 5′-DY682-labeled DNA fragments were purchased from Eurofins MWG Operon.

ChIP-PCR

ChIP-qPCR was performed with 2-week-old Arabidopsis seedlings expressing functional GFP-tagged ATAF1 protein from the 35S promoter (*35S:ATAF1-GFP*) using anti-GFP antibody to immunoprecipitate protein-DNA complexes as reported (Kaufmann et al., 2010; Wu et al., 2012). Col-0 plants served as negative controls. Primers used for qPCR flanked the ATAF1 binding site within the promoter region of *TRE1*. Primers annealing to promoter regions of an Arabidopsis gene (*CLAVATA1*; *At1g75820*) lacking an ATAF1 binding site were used in negative control experiments. The ChIP experiment was run in two biological replications with three technical repetitions per assay. ChIP-qPCR data were analyzed as described (Wu et al., 2012).

Determination of Trehalase Activity

Three replicates of at least 30 seedlings were frozen in liquid nitrogen and homogenized. The powdered tissue (100 mg) was extracted in 1 mL of ice-cold protein extraction buffer (0.1 M MES-KOH, pH 6, 1 mM EDTA, 1 mM phenylmethylsulfonyl fluoride, 1% [w/v] polyvinylpyrrolidone, and 1 mM dithiothreitol) containing protease inhibitors (Complete EDTA-Free; Roche). The suspension was cleared by centrifugation (18,000*g* at 4°C for 10 min). Trehalase activity was determined as described previously (Pernambuco et al., 1996) with minor modifications. Aliquots of the protein extract were incubated in the reaction buffer (62.5 mM MES-KOH, pH 7 and 125 μM $CaCl_2$) containing 250 mM trehalose. The Glc released was quantified using the GLC (GO) Assay Kit (GAGO-20; Sigma-Aldrich). Control reactions were performed by incubating the protein extracts in reaction buffer without trehalose. This allowed measurement of the Glc level in the protein extract, which was subtracted from the Glc released because of trehalase activity in samples incubated with trehalose. The protein concentrations were determined according to the work by Bradford (1976) with bovine serum albumin as standard. The Glc levels were normalized against the protein concentration to determine the specific activity.

Western-Blot Analysis of TRE1

Two-week-old seedlings were harvested, frozen in liquid nitrogen, and homogenized. The powdered tissue (100 mg) was extracted in 1 mL of ice-cold protein extraction buffer. After centrifugation at 14,000*g* for 15 min, soluble proteins were collected, and concentrations were determined using the assay by Bradford (1976). For each sample, aliquots containing 20 μg of protein were analyzed by SDS-PAGE on duplicate 12% polyacrylamide gels. One gel was stained with 0.25% Coomassie Brilliant Blue R250 as a sample loading control, and proteins from the other gel were electroblotted onto Protran Nitrocellulose Membrane (Whatman) for immunological analysis. The membrane was blocked for 1 h in blocking buffer (5% nonfat dry milk in phosphate-buffered saline containing 0.1% Tween 20) followed by incubation for 1 h with polyclonal rabbit anti-TRE1 antibody (1:1,000 dilution) as a primary antibody. After washing, the membrane was incubated with IRDye 800CW donkey anti-rabbit IgG secondary antibody (1:10,000 dilution; Li-Cor) for 60 min at room temperature with constant shaking. Signal intensities were analyzed at 800 nm using an Odyssey Infrared Imaging System (Li-Cor).

Quantification of Starch and Soluble Sugars

Suc, Glc, and Fru were extracted with ethanol (Scheible et al., 1997) and quantified enzymatically according to Stitt et al., 1989. Starch was determined enzymatically in the pellets obtained after ethanol extraction of soluble sugars (Hendriks et al., 2003).

Quantification of Primary Metabolites

Tre6P and phosphorylated intermediates were extracted in chloroform-methanol and measured by high-performance anion-exchange chromatography coupled to tandem mass spectrometry as described in Lunn et al., 2006 using a QTrap 5500 MS-Q3 (AB Sciex) Triple Quadrupole Mass Spectrometer. Tre6P was quantified using enzymatically calibrated standards and an [^{2}H] Tre6P internal standard to correct for ion suppression and matrix effects (Lunn et al., 2006). Trehalose was quantified fluorimetrically as described by Carillo et al. (2013) in the same chloroform-methanol extract used for Tre6P determination.

Microscopy

Presence of ATAF1-GFP fusion protein in transgenic plants was analyzed by confocal fluorescence microscopy (Eclipse E600 Microscope; Nikon).

Treatments

[AU : 37] For ESTR induction, 2-week-old seedlings were incubated in liquid full-strength Murashige and Skoog medium containing 1% (w/v) Suc and 10 μM ESTR (dissolved in 0.1% [v/v] ethanol; control: 0.1% ethanol) and kept on a rotary shaker for 1, 2, 5, or 10 h until harvest. Gene expression was determined by qRT-PCR. For trehalose and validamycin A treatment, 12-d-old seedlings were transferred to solid one-half-strength Murashige and Skoog medium supplemented with trehalose (25 mM) or trehalose (25 mM) and validamycin A (10 μM) and grown for 2 weeks.

[AU : 38] AGI Codes

[AU : 39] AGI codes are *ACTIN2* (At3g18780), *ATAF1* (At1g01720), *BAM3* (At4g17090), *STP1* (At1g11260), *TPS1* (At1g78580), and *TRE1* (At4g24040; additional AGI codes are given in Supplemental Tables S1–S7).

[AU : 40] Sequence data from this article can be found in the GenBank/EMBL data libraries under accession numbers.

Supplemental Data

[AU : 41] The following supplemental materials are available.

Supplemental Figure S1.

Supplemental Figure S2.

Supplemental Figure S3.

Supplemental Figure S4.

Supplemental Table S1.

Supplemental Table S2.

Supplemental Table S3.

Supplemental Table S4.

Supplemental Table S5.

Supplemental Table S6.

Supplemental Table S7.

ACKNOWLEDGMENTS

We thank Karin Koehl and team for plant care and Sandhya Yellina for expression and purification of ATAF1 protein.

Received June 18, 2015; accepted July 2, 2015; published July 6, 2015.

LITERATURE CITED

Allu AD, Soja AM, Wu A, Szymanski J, Balazadeh S (2014) Salt stress and senescence: identification of cross-talk regulatory components. J Exp Bot **65:** 3993–4008

Araújo WL, Ishizaki K, Nunes-Nesi A, Larson TR, Tohge T, Krahnert I, Witt S, Obata T, Schauer N, Graham IA, et al (2010) Identification of the 2-hydroxyglutarate and isovaleryl-CoA dehydrogenases as alternative electron donors linking lysine catabolism to the electron transport chain of *Arabidopsis* mitochondria. Plant Cell **22:** 1549–1563

Araújo WL, Ishizaki K, Nunes-Nesi A, Tohge T, Larson TR, Krahnert I, Balbo I, Witt S, Dörmann P, Graham IA, et al (2011) Analysis of a range of catabolic mutants provides evidence that phytanoyl-coenzyme A does not act as a substrate of the electron-transfer flavoprotein/electron-transfer flavoprotein:ubiquinone oxidoreductase complex in Arabidopsis during dark-induced senescence. Plant Physiol **157:** 55–69

Avin-Wittenberg T, Bajdzienko K, Wittenberg G, Alseekh S, Tohge T, Bock R, Giavalisco P, Fernie AR (2015) Global analysis of the role of autophagy in cellular metabolism and energy homeostasis in *Arabidopsis* seedlings under carbon starvation. Plant Cell **27:** 306–322

Avonce N, Mendoza-Vargas A, Morett E, Iturriaga G (2006) Insights on the evolution of trehalose biosynthesis. BMC Evol Biol **6:** 109

Baena-González E, Rolland F, Thevelein JM, Sheen J (2007) A central integrator of transcription networks in plant stress and energy signalling. Nature **448:** 938–942

Balazadeh S, Riaño-Pachón DM, Mueller-Roeber B (2008) Transcription factors regulating leaf senescence in *Arabidopsis thaliana*. Plant Biol (Stuttg) (Suppl 1) **10:** 63–75

Balazadeh S, Siddiqui H, Allu AD, Matallana-Ramirez LP, Caldana C, Mehrnia M, Zanor MI, Köhler B, Mueller-Roeber B (2010) A gene regulatory network controlled by the NAC transcription factor ANAC092/AtNAC2/ORE1 during salt-promoted senescence. Plant J **62:** 250–264

Bläsing OE, Gibon Y, Günther M, Höhne M, Morcuende R, Osuna D, Thimm O, Usadel B, Scheible WR, Stitt M (2005) Sugars and circadian regulation make major contributions to the global regulation of diurnal gene expression in *Arabidopsis*. Plant Cell **17:** 3257–3281

Blázquez MA, Santos E, Flores CL, Martínez-Zapater JM, Salinas J, Gancedo C (1998) Isolation and molecular characterization of the *Arabidopsis TPS1* gene, encoding trehalose-6-phosphate synthase. Plant J **13:** 685–689

Bradford MM (1976) A rapid and sensitive method for the quantitation of microgram quantities of protein utilizing the principle of protein-dye binding. Anal Biochem **72:** 248–254

Caldana C, Scheible WR, Mueller-Roeber B, Ruzicic S (2007) A quantitative RT-PCR platform for high-throughput expression profiling of 2500 rice transcription factors. Plant Methods **3:** 7

Carillo P, Feil R, Gibon Y, Satoh-Nagasawa N, Jackson D, Bläsing OE, Stitt M, Lunn JE (2013) A fluorometric assay for trehalose in the picomole range. Plant Methods **9:** 21–35

Contento AL, Kim SJ, Bassham DC (2004) Transcriptome profiling of the response of Arabidopsis suspension culture cells to Suc starvation. Plant Physiol **135:** 2330–2347

Delatte TL, Sedijani P, Kondou Y, Matsui M, de Jong GJ, Somsen GW, Wiese-Klinkenberg A, Primavesi LF, Paul MJ, Schluepmann H (2011) Growth arrest by trehalose-6-phosphate: an astonishing case of primary metabolite control over growth by way of the SnRK1 signaling pathway. Plant Physiol **157:** 160–174

Delorge I, Figueroa CM, Feil R, Lunn JE, Van Dijck P (2015) Trehalose-6-phosphate synthase 1 is not the only active TPS in *Arabidopsis thaliana*. Biochem J **466:** 283–290

Dortay H, Schmöckel SM, Fettke J, Mueller-Roeber B (2011) Expression of human c-reactive protein in different systems and its purification from *Leishmania tarentolae*. Protein Expr Purif **78:** 55–60

Du Z, Zhou X, Ling Y, Zhang Z, Su Z (2010) agriGO: a GO analysis toolkit for the agricultural community. Nucleic Acids Res **38:** W64–W70

Ekkehard Neuhaus H, Stitt M (1990) Control analysis of photosynthate partitioning: impact of reduced activity of ADP-glucose pyrophosphorylase or plastid phosphoglucomutase on the fluxes to starch and sucrose in *Arabidopsis thaliana* (L.) Heynh. Planta **182:** 445–454

Ernst J, Bar-Joseph Z (2006) STEM: a tool for the analysis of short time series gene expression data. BMC Bioinformatics **7:** 191

Frison M, Parrou JL, Guillaumot D, Masquelier D, François J, Chaumont F, Batoko H (2007) The *Arabidopsis thaliana* trehalase is a plasma membrane-bound enzyme with extracellular activity. FEBS Lett **581:** 4010–4016

Garapati P, Xue GP, Munné-Bosch S, Balazadeh S (2015) Transcription factor ATAF1 in Arabidopsis promotes senescence by direct regulation of key chloroplast maintenance and senescence transcriptional cascades. Plant Physiol **168:** 1122–1139

Gentleman RC, Carey VJ, Bates DM, Bolstad B, Dettling M, Dudoit S, Ellis B, Gautier L, Ge Y, Gentry J, et al (2004) Bioconductor: open software development for computational biology and bioinformatics. Genome Biol **5:** R80

Halford NG, Hey SJ (2009) Snf1-related protein kinases (SnRKs) act within an intricate network that links metabolic and stress signalling in plants. Biochem J **419:** 247–259

Hendriks JH, Kolbe A, Gibon Y, Stitt M, Geigenberger P (2003) ADP-glucose pyrophosphorylase is activated by posttranslational redox-modification in response to light and to sugars in leaves of Arabidopsis and other plant species. Plant Physiol **133:** 838–849

Ishizaki K, Schauer N, Larson TR, Graham IA, Fernie AR, Leaver CJ (2006) The mitochondrial electron transfer flavoprotein complex is essential for survival of *Arabidopsis* in extended darkness. Plant J **47:** 751–760

Izumi M, Hidema J, Makino A, Ishida H (2013) Autophagy contributes to nighttime energy availability for growth in Arabidopsis. Plant Physiol **161:** 1682–1693

Jensen MK, Hagedorn PH, de Torres-Zabala M, Grant MR, Rung JH, Collinge DB, Lyngkjaer MF (2008) Transcriptional regulation by an NAC (NAM-ATAF1,2-CUC2) transcription factor attenuates ABA signalling for efficient basal defence towards *Blumeria graminis* f. sp. hordei in *Arabidopsis*. Plant J **56:** 867–880

Jensen MK, Lindemose S, de Masi F, Reimer JJ, Nielsen M, Perera V, Workman CT, Turck F, Grant MR, Mundy J, et al (2013) ATAF1 transcription factor directly regulates abscisic acid biosynthetic gene *NCED3* in *Arabidopsis thaliana*. FEBS Open Bio **3:** 321–327

Kaufmann K, Muiño JM, Østerås M, Farinelli L, Krajewski P, Angenent GC (2010) Chromatin immunoprecipitation (ChIP) of plant transcription factors followed by sequencing (ChIP-SEQ) or hybridization to whole genome arrays (ChIP-CHIP). Nat Protoc **5:** 457–472

Kim JH, Woo HR, Kim J, Lim PO, Lee IC, Choi SH, Hwang D, Nam HG (2009) Trifurcate feed-forward regulation of age-dependent cell death involving *miR164* in *Arabidopsis*. Science **323:** 1053–1057

Kleinow T, Himbert S, Krenz B, Jeske H, Koncz C (2009) NAC domain transcription factor ATAF1 interacts with SNF1-related kinases and silencing of its subfamily causes severe developmental defects in *Arabidopsis*. Plant Sci **177:** 360–370 [**AU : 42**]

Leyman B, Van Dijck P, Thevelein JM (2001) An unexpected plethora of trehalose biosynthesis genes in *Arabidopsis thaliana*. Trends Plant Sci **6:** 510–513

Lin JF, Wu SH (2004) Molecular events in senescing Arabidopsis leaves. Plant J **39:** 612–628

Lu PL, Chen NZ, An R, Su Z, Qi BS, Ren F, Chen J, Wang XC (2007) A novel drought-inducible gene, *ATAF1*, encodes a NAC family protein that negatively regulates the expression of stress-responsive genes in *Arabidopsis*. Plant Mol Biol **63:** 289–305

Lunn JE (2007) Compartmentation in plant metabolism. J Exp Bot **58:** 35–47

Lunn JE, Delorge I, Figueroa CM, Van Dijck P, Stitt M (2014) Trehalose metabolism in plants. Plant J **79:** 544–567

Lunn JE, Feil R, Hendriks JH, Gibon Y, Morcuende R, Osuna D, Scheible WR, Carillo P, Hajirezaei MR, Stitt M (2006) Sugar-induced increases in trehalose 6-phosphate are correlated with redox activation of ADP-glucose pyrophosphorylase and higher rates of starch synthesis in *Arabidopsis thaliana*. Biochem J **397:** 139–148

Ma J, Hanssen M, Lundgren K, Hernández L, Delatte T, Ehlert A, Liu CM, Schluepmann H, Dröge-Laser W, Moritz T, et al (2011) The sucrose-regulated *Arabidopsis* transcription factor bZIP11 reprograms metabolism and regulates trehalose metabolism. New Phytol **191:** 733–745

Martins MC, Hejazi M, Fettke J, Steup M, Feil R, Krause U, Arrivault S, Vosloh D, Figueroa CM, Ivakov A, et al (2013) Feedback inhibition of starch degradation in Arabidopsis leaves mediated by trehalose 6-phosphate. Plant Physiol **163:** 1142–1163

Miyashita Y, Good AG (2008) Glutamate deamination by glutamate dehydrogenase plays a central role in amino acid catabolism in plants. Plant Signal Behav **3:** 842–843

Müller J, Aeschbacher RA, Wingler A, Boller T, Wiemken A (2001) Trehalose and trehalase in Arabidopsis. Plant Physiol **125:** 1086–1093

Nunes C, O'Hara LE, Primavesi LF, Delatte TL, Schluepmann H, Somsen GW, Silva AB, Fevereiro PS, Wingler A, Paul MJ (2013) The trehalose 6-phosphate/SnRK1 signaling pathway primes growth recovery following relief of sink limitation. Plant Physiol **162:** 1720–1732

Osuna D, Usadel B, Morcuende R, Gibon Y, Bläsing OE, Höhne M, Günter M, Kamlage B, Trethewey R, Scheible WR, et al (2007) Temporal responses of transcripts, enzyme activities and metabolites after adding sucrose to carbon-deprived *Arabidopsis* seedlings. Plant J **49:** 463–491

Paul MJ, Jhurreea D, Zhang Y, Primavesi LF, Delatte T, Schluepmann H, Wingler A (2010) Upregulation of biosynthetic processes associated with growth by trehalose 6-phosphate. Plant Signal Behav **5:** 386–392

Pernambuco MB, Winderickx J, Crauwels M, Griffioen G, Mager WH, Thevelein JM (1996) Glucose-triggered signalling in *Saccharomyces cerevisiae*: different requirements for sugar phosphorylation between cells grown on glucose and those grown on non-fermentable carbon sources. Microbiology **142:** 1775–1782

Ramon M, Rolland F, Thevelein JM, Van Dijck P, Leyman B (2007) ABI4 mediates the effects of exogenous trehalose on *Arabidopsis* growth and starch breakdown. Plant Mol Biol **63:** 195–206

Rose TL, Bonneau L, Der C, Marty-Mazars D, Marty F (2006) Starvation-induced expression of autophagy-related genes in *Arabidopsis*. Biol Cell **98:** 53–67

Scheible WR, González-Fontes A, Morcuende R, Lauerer M, Geiger M, Glaab J, Gojon A, Schulze ED, Stitt M (1997) Tobacco mutants with a decreased number of functional *nia* genes compensate by modifying the diurnal regulation of transcription, post-translational modification and turnover of nitrate reductase. Planta **203:** 304–319

Schluepmann H, Berke L, Sanchez-Perez GF (2012) Metabolism control over growth: a case for trehalose-6-phosphate in plants. J Exp Bot **63:** 3379–3390

Schluepmann H, Pellny T, van Dijken A, Smeekens S, Paul M (2003) Trehalose 6-phosphate is indispensable for carbohydrate utilization and growth in *Arabidopsis thaliana*. Proc Natl Acad Sci USA **100:** 6849–6854

Schluepmann H, van Dijken A, Aghdasi M, Wobbes B, Paul M, Smeekens S (2004) Trehalose mediated growth inhibition of Arabidopsis seedlings is due to trehalose-6-phosphate accumulation. Plant Physiol **135:** 879–890

Skirycz A, Reichelt M, Burow M, Birkemeyer C, Rolcik J, Kopka J, Zanor MI, Gershenzon J, Strnad M, Szopa J, et al (2006) DOF transcription factor AtDof1.1 (OBP2) is part of a regulatory network controlling glucosinolate biosynthesis in *Arabidopsis*. Plant J **47:** 10–24

Stitt M, Lilley RM, Gerhardt R, Heldt HW (1989) Metabolite levels in specific cells and subcellular compartments of plant leaves. Methods Enzymol **174:** 518–552 [**AU : 43**]

Thimm O, Bläsing O, Gibon Y, Nagel A, Meyer S, Krüger P, Selbig J, Müller LA, Rhee SY, Stitt M (2004) MAPMAN: a user-driven tool to

display genomics data sets onto diagrams of metabolic pathways and other biological processes. Plant J **37:** 914–939

Tsai AY, Gazzarrini S (2012) AKIN10 and FUSCA3 interact to control lateral organ development and phase transitions in *Arabidopsis*. Plant J **69:** 809–821

Usadel B, Bläsing OE, Gibon Y, Retzlaff K, Höhne M, Günther M, Stitt M (2008) Global transcript levels respond to small changes of the carbon status during progressive exhaustion of carbohydrates in Arabidopsis rosettes. Plant Physiol **146:** 1834–1861

Vandesteene L, López-Galvis L, Vanneste K, Feil R, Maere S, Lammens W, Rolland F, Lunn JE, Avonce N, Beeckman T, et al (2012) Expansive evolution of the TREHALOSE-6-PHOSPHATE PHOSPHATASE gene family in Arabidopsis. Plant Physiol **160:** 884–896

Van Houtte H, Vandesteene L, López-Galvis L, Lemmens L, Kissel E, Carpentier S, Feil R, Avonce N, Beeckman T, Lunn JE, Van Dijck P (2013) Overexpression of the trehalase gene *AtTRE1* leads to increased drought stress tolerance in Arabidopsis and is involved in abscisic acid-induced stomatal closure. Plant Physiol **161:** 1158–1171

Vigeolas H, Möhlmann T, Martini N, Neuhaus HE, Geigenberger P (2004) Embryo-specific reduction of ADP-Glc pyrophosphorylase leads to an inhibition of starch synthesis and a delay in oil accumulation in developing seeds of oilseed rape. Plant Physiol **136:** 2676–2686

Waters MT, Moylan EC, Langdale JA (2008) GLK transcription factors regulate chloroplast development in a cell-autonomous manner. Plant J **56:** 432–444

Waters MT, Wang P, Korkaric M, Capper RG, Saunders NJ, Langdale JA (2009) GLK transcription factors coordinate expression of the photosynthetic apparatus in *Arabidopsis*. Plant Cell **21:** 1109–1128

Wingler A, Fritzius T, Wiemken A, Boller T, Aeschbacher RA (2000) Trehalose induces the ADP-glucose pyrophosphorylase gene, *ApL3*, and starch synthesis in Arabidopsis. Plant Physiol **124:** 105–114

Wu A, Allu AD, Garapati P, Siddiqui H, Dortay H, Zanor MI, Asensi-Fabado MA, Munné-Bosch S, Antonio C, Tohge T, et al (2012) *JUNGBRUNNEN1*, a reactive oxygen species-responsive NAC transcription factor, regulates longevity in *Arabidopsis*. Plant Cell **24:** 482–506

Wu Y, Deng Z, Lai J, Zhang Y, Yang C, Yin B, Zhao Q, Zhang L, Li Y, Yang C, et al (2009) Dual function of *Arabidopsis* ATAF1 in abiotic and biotic stress responses. Cell Res **19:** 1279–1290

Wu ZJ, Irizarry RA, Gentleman R, Martinez-Murillo F, Spencer F (2004) A model-based background adjustment for oligonucleotide expression arrays. J Am Stat Assoc **99:** 909–917 [**AU : 44**]

Xue GP (2005) A CELD-fusion method for rapid determination of the DNA-binding sequence specificity of novel plant DNA-binding proteins. Plant J **41:** 638–649

Yadav UP, Ivakov A, Feil R, Duan GY, Walther D, Giavalisco P, Piques M, Carillo P, Hubberten HM, Stitt M, et al (2014) The sucrose-trehalose 6-phosphate (Tre6P) nexus: specificity and mechanisms of sucrose signalling by Tre6P. J Exp Bot **65:** 1051–1068

Zhang Y, Primavesi LF, Jhurreea D, Andralojc PJ, Mitchell RA, Powers SJ, Schluepmann H, Delatte T, Wingler A, Paul MJ (2009) Inhibition of SNF1-related protein kinase1 activity and regulation of metabolic pathways by trehalose-6-phosphate. Plant Physiol **149:** 1860–1871

Zuo J, Niu QW, Chua NH (2000) Technical advance: an estrogen receptor-based transactivator XVE mediates highly inducible gene expression in transgenic plants. Plant J **24:** 265–273

QUERIES -ppPP201500917

[AU: QA1] If you provided an ORCID ID at submission, please confirm that it appears correctly on the opening page of this article. If you or your coauthors would like to include an ORCID ID in this publication, please provide it with your corrections. If you do not have an ORCID ID and would like one, you can register for your unique digital identifier at https://orcid.org/register.

[AU: 1] Please spell out ATAF1 in the title.

[AU: 2] Please spell out VIB and KU in the affiliations.

[AU: 3] Please spell out FOR in footnote 1.

[AU: 4] Is distribution of materials information correct as shown? Please confirm or amend. (Only one name may be listed.)

[AU: 5] Please review the following Table of Contents summary text and edit to avoid acronyms or abbreviations: "*The transcription factor ATAF1 from Arabidopsis regulates TREHALASE1 expression and induces a carbon starvation transcriptome and metabolome*."

[AU: 6] Please spell out NAC in the abstract.

[AU: 7] Please spell out ATAF1 here, followed by the abbreviation in parentheses.

[AU: 8] Please spell out Snf1 here, followed by the abbreviation in parentheses.

[AU: 9] Please spell out KIN10 here, followed by the abbreviation in parentheses.

[AU: 10] Please spell out NAC, ABI3VP1, and FUSCA3 in the text.

[AU: 11] Please spell out ATAF1 here, followed by the abbreviation in parentheses.

[AU: 12] Please verify abscisic acid for ABA here.

[AU: 13] Please spell out NCED3 here, followed by the abbreviation in parentheses.

[AU: 14] Please spell out ORE1 and GLK1here, followed by the abbreviations in parentheses.

[AU: 15] Please spell out ANAC092 in the text.

[AU: 16] Please spell out IOE here, followed by the abbreviation in parentheses.

[AU: 17] Please spell out ATH1 here, followed by the abbreviation in parentheses.

[AU: 18] Please verify quantitative reverse transcription for qRT here.

[AU: 19] Please verify transfer DNA for T-DNA here and below.

[AU: 20] Please spell out GABI-Kat in the text.

[AU: 21] Please spell out EMSA here, followed by the abbreviation in parentheses.

[AU: 22] Please verify double-stranded DNA for dsDNA here.

[AU: 23] Please spell out APL3 here, followed by the abbreviation in parentheses.

[AU: 24] Please spell out GBSS1, SS3, BE1, ISA2/DBE1, and GWD in the text.

[AU: 25] Please spell out bZIP11 here, followed by the abbreviation in parentheses.

[AU: 26] Per journal style, ppm was changed to μL L^{-1} here. Please verify.

[AU: 27] Please verify Columbia-0 for Col-0 here.

[AU: 28] Please spell out GO here, followed by the abbreviation in parentheses.

[AU: 29] Please spell out ATG3 here, followed by the abbreviation in parentheses.

[AU: 30] Please verify that each Web site given in this article can still be accessed; if not, please provide necessary corrections.

[AU: 31] Please define % concentrations throughout as (w/w), (w/v), or (v/v).

[AU: 32] Please verify full-strength for 1x here and below.

[AU: 33] Please spell out CEL in the text.

[AU: 34] Please spell out GCRMA in the text.

[AU: 35] Please spell out CELD and pLysS in the text.

[AU: 36] Please verify phenylmethylsulfonyl fluoride for PMSF and dithiothreitol for DTT here.

[AU: 37] Please verify Murashige and Skoog medium for MS here and below.

[AU: 38] Please spell out AGI here.

[AU: 39] Please spell out AGI in the text.

[AU: 40] Journal style requires that accession numbers be listed in this manner. Please provide appropriate number or delete if unnecessary.

[AU: 41] Please provide short titles for all supplemental materials listed here.

[AU: 42] Please verify reference information in reference Kleinow et al.

[AU: 43] Please verify reference information in reference Stitt et al.

[AU: 44] Please verify reference information in reference Wu et al. (2004).

[AU: 45] Please define CLV1, NC, and CELD in Figure 1 legend.

[AU: 46] Please verify A-C in Figure 2 legend.

[AU: 47] Please verify fresh weight for FW here and below.

[AU: 48] Please define GBSS1, ATSS3, BE1, DBE1, GWD3/PWD, and SAG29 in Figure 3 legend.

[AU: 49] Please define all gene names not defined in the text in Figure 4 legend.